CHARACTERISTICS OF RF-DRIVEN STEADY STATE TOKAMAK POWER REACTORS

S.Y. Yuen, D. Kaplan, D.R. Cohn

April 1979
M.I.T. Plasma Fusion Center Report #RR-79-7

CHARACTERISTICS OF RF-DRIVEN STEADY STATE TOKAMAK POWER REACTORS[+]

S. Y. Yuen, D. Kaplan[++], D.R. Cohn
M.I.T. Plasma Fusion Center[*]
and
Frances Bitter National Magnet Laboratory[**]

[+]Work supported by U.S. Department of Energy Contract ET-78-S-02-4646.

[++]Present address: Energy, Inc., Richmond, VA
[*]Supported by D.O.E.
[**]Supported by N.S.F.

ABSTRACT

The use of lower hybrid waves for current drive in steady state tokamak power reactors is studied. Constraints imposed by rf wave propagation are considered in detail. The effect of decoupling of electron and ion temperatures is studied and is found to enhance significantly the ratio of fusion power to dissipated power. Tradeoffs for parameters of rf driven steady state reactors are determined. It is found that rf driven steady state current operation is especially suitable for high field reactor designs. For example, our study indicates that a tokamak power reactor characterized by a major radius of 6 meters, a magnetic field on axis of 7.5 T, and a thermal output power of 2500 MW could be driven in steady state operation with rf power level equal to 4.3% of the fusion power output.

I. INTRODUCTION

The use of radio frequency (rf) waves near the lower hybrid frequency to drive a steady state electron current in tokamaks has been proposed recently [1,2]. In the proposed scheme, a continuous current is generated by electron Landau damping of rf waves traveling in only one direction parallel to the magnetic field. The wave carries net parallel momentum, which, when absorbed by resonant electrons, drives the toroidal current for plasma confinement. With this scheme steady state tokamak operation becomes possible. This mode of operation has several advantages over pulsed operation. First wall thermal fatique would be reduced, eddy current effects caused by start-up and shutdown would be mitigated, and a thermal "flywheel" would become unnecessary. In addition, smaller aspect ratio designs are possible because of the reduced volt-second requirements. Moreover, the rf radiation could be used to heat the plasma to near ignition conditions, and also be used to control the thermal stability of the reactor.

The use of rf current drive in tokamak power reactors has been studied before [2,3]. Ignoring all plasma profile effects, Fisch made a rough estimate for a tokamak power reactor with UWMAK-I parameters (major radius R = 13 m, minor radius a = 5 m), and found that a low ratio of circulating rf power to fusion power can easily be achieved [2]. Ehst took into account tokamak density, temperature and current profiles, and found it possible to drive the current of a moderate size tokamak power reactor (R = 7 m) with a low ratio of circulating rf power to fusion power [3]. However, the currents generated were surface currents and although such

currents are shown to be consistent with magnetohydrodynamic equilibria [3], the stability of such equilibria is questionable.

Previous studies of lower hybrid wave driven steady state tokamak power reactors did not fully take into account the accessibility criteria of the lower hybrid wave. These studies [2,3] also ignored the counter streaming current carried by the non-resonant electrons. This is a good approximation for low temperature plasmas, but cannot be used for elevated temperatures characteristic of reactor plasmas. In addition, in previous studies the electron and ion temperatures were assumed to be equal, which is in general not true for ignited tokamak plasmas.

This paper includes the additional effects described above. These effects significantly modify the conclusion of the previous studies and lead to a new frame of reference for assessing rf current drive in tokamak power reactors. Details of lower hybrid wave propagation are taken into account, including accessibility, linear mode conversation, non-linear instability, variation of parallel phase velocity in toroidal geometry, and the variation of rf wave spectrum as the wave travels into the plasma with a variety of density and temperature profiles. Particular attention is given in this paper to the effect of ion-electron temperature decoupling at ignition [4], [5]. Operation in the decoupled ion-electron regime will enhance the fusion to rf power ratio since more fusion power is produced at higher T_i, while the dissipated rf power is kept low with low T_e. The fusion to rf power ratio would further increased if the alpha particle energy is anomalously transferred to the ions [6], thereby increasing the ion-electron temperature decoupling.

Section II of this paper briefly discusses the quasi-linear theory for current generation and presents some modifications to previous results. Section III considers the propagation of lower hybrid waves in the tokamak plasma. In Section IV characteristics of nearly ignited plasmas are presented. Section V discusses the effectiveness of rf driven steady state operation and reactor parameter tradeoffs. The main results of the paper are summarized in Section VI.

II. QUASI-LINEAR THEORY FOR CURRENT GENERATION

Consider an rf wave with energy $\mathcal{E}$, parallel phase velocity v_z, and frequency ω traveling in a plasma with electron temperature T_e and density n_e. The wave distorts the electron distribution and produces a plateau in the region of resonant particles. However, binary collisions of the resonant particles with other plasma particles tends to restore thermal equilibrium, thus establishing stationary wave absorption. On the other hand, since the wave travels in only one direction, the asymmetric electron distribution thus created will result in a net current in the direction of the wave's phase velocity.

After averaging over velocities perpendicular to the magnetic field, the one dimensional quasi-linear equation for an electron distribution function f in the presence of rf field is given by [7].

$$\frac{\partial f}{\partial \tau} = \frac{\partial}{\partial u}\left[\left(D + \frac{1}{2u^3}\right)\frac{\partial f}{\partial u} + \frac{f}{u^2}\right] \tag{1}$$

where $u \equiv v_z/v_{Te}$, $v_{Te} = (2T_e/m_e)^{1/2}$, $\tau = \nu u^3 t$, $\nu = 2\pi(Z_i + 3)n_e e^4 \ell n \Lambda / m_e^2 v_z^3$, and $D = D_{QL}/\nu u^3 v_{Te}^2 \simeq [4\pi/(Z_i + 3)](1/n_e e^4 \ell n \Lambda u)[\mathcal{E}_{kz}/\partial(\varepsilon_R \omega)/\partial\omega]$. D_{QL} is the quasi-linear diffusion coefficient, Z_i the charge of the ion species, and ε_R the real part of the dielectric function of the lower hybrid wave. In the steady state, the electron flux in velocity space vanishes, and the solution of Eq.(1) is given by

$$f(u) = \begin{cases} \dfrac{1}{\sqrt{\pi}}\, e^{-u_1^2}\left[\dfrac{2D_0 u_1^2 + 1}{2D_0 u^2 + 1}\right]^{D_0/2} & u_1 \le u \le u_2 \\ f_m(u) = \dfrac{1}{\sqrt{\pi}}\, e^{-u^2} & u < u_1 \ , \quad u > u_2 \end{cases} \tag{2}$$

where $D_0 = Du$ and the rf wave spectrum is assumed to be

$$\mathcal{E}_{kz} = \mathcal{E}/\Delta k_z \qquad u_1 \le u \le u_2 \tag{3}$$

and zero elsewhere, $\Delta k_z = k_{z_1} - k_{z_2} = (\omega/u_1 - \omega/u_2)/v_{Te}$.

The current density generated can at once be obtained from Eq.(2) by integrating over velocity space

$$J = \frac{1}{2} n_e e v_{Te} f_m(u_1) K \left\{ \frac{(2D_0 u_1^2 + 1)^{D_0/2}}{(2D_0 - 1)} \left[(2D_0 u_2^2 + 1)^{1-1/2D_0} - (2D_0 u_1^2 + 1)^{1-1/2D_0} - \exp(u_1^2 - u_2^2) + 1 \right] \right\} \tag{4}$$

which, when $D_0 >> 1$, reduces to

$$J = \frac{1}{2} n_e e v_{Te} f_m(u_1) K \left[u_2^2 - u_1^2 - \exp(u_1^2 - u_2^2) + 1 \right] \tag{5}$$

Note that a constant, K, appears in Eqs. (4) and (5). This constant is a correction factor that arises from the approximations made in the one-dimensional analysis. By numerically solving the two-dimensional Fokker-Planck equation with a quasi-linear diffusion term, it has been found that K = 1.6 [8]. The last two terms in Eq. (5) account for the counter streaming current contributed by electrons with velocity $-u_2 < u < -u_1$. Figure 1 shows the ratio of Eq. (5) to the approximate result J_F of Refs. [1,2] where the counter streaming current was neglected. With typical reactor parameters, T_e = 18 KeV, parallel refractive index n_z = 1.7, u_1 = 2.2, u_2/u_1 = 1.1 - 1.2, a discrepancy factor of 0.34 - 0.58 is found between the two results. This implies that the results of previous studies of rf driven steady state

tokamak which ignored the counter streaming current [2][3] are overly optimistic. In some of the high temperature plasmas, electrons may become relativistic at the plasma center. Relativistic effects are not included in the present study. However, a rough estimate including relativistic effects with T_e = 18 KeV u_1 = 2.2, u_2/u_1 = 1.2, (u_1/c = 0.58), gives a current density about 47% less than Eq. (5). On the other hand, the rf power dissipated also decreases by $\sim$ 64% from Eq. (9). Thus relativistic effects introduces a net gain in J/P_D for this case.

The variation of rf field energy density as it penetrates radially into the plasma can be easily derived from quasi-linear results [7]

$$\frac{\partial}{\partial r}(v_{g\perp}\mathcal{E}_{kz}) = -2\,\gamma_{kz}\mathcal{E}_{kz} \tag{6}$$

$$\gamma_{kz} = \frac{\gamma_{okz}}{1+2Du^3} = \sqrt{\frac{\pi}{8}}\,\frac{\omega^2}{(1+\omega_{pe}^2/\Omega_e^2)\,\omega_{pe}(k_z\lambda_D)^3}\,\frac{1}{1+2Du^3}\,e^{-u^2} \tag{7}$$

Here, γ_{kz} is the quasi-linear corrected damping rate, $v_{g\perp} = \partial\omega/\partial k_\perp$ is the perpendicular group velocity, ω_{pe}, Ω_e the electron plasma and cyclotron frequencies and λ_D the Debye wavelength. All of these quantities are a function of r through density, temperature and magnetic field profiles. The power density dissipated by the rf wave with spectral width $\Delta k_z = k_{z1} - k_{z2}$ is given by

$$P_D = \int_{k_{z_2}}^{k_{z_1}} 2\gamma_{kz}\mathcal{E}_{kz}\,dk_z \quad . \tag{8}$$

When $Du^3 \gg 1$, Eq. (8) can be approximated as

$$P_D = \frac{1}{2}\nu u_1^3\, v_{Te}^2 n_e m_e (\partial\varepsilon_R\omega/\partial\omega) f_m(u_1)\ell n(u_2/u_1) \tag{9}$$

which is the same result derived in Refs. [1,2].

The ratio of current generated to power dissipated, J/P_D, indicates the effectiveness of rf generated current. From Eqs. (5) and (9), Fig. 2 plots J/P_D for various values of u_1 and u_2. As can be seen J/P_D varies rather rapidly as u_1 and u_2. Furthermore it is apparent that high phase velocity waves are far more effective in generating current than low phase velocity waves. However, the maximum phase velocity of lower hybrid waves allowed in a plasma is limited by the accessibility criterion among other constraints. Thus it is important to examine the constraints on the rf wave phase velocities as imposed by wave-plasma interaction.

III. PROPAGATION OF LOWER HYBRID WAVE

Consider a slow wave launched at the edge of the plasma torous. The lower hybrid wave will propagate in a resonance cone with local perpendicular wave number $k_\perp = k_z (-\varepsilon_3/\varepsilon_1)^{1/2}$, $\varepsilon_3 = 1 - (\omega_{pe}/\omega)^2$, $\varepsilon_1 = 1 + (\omega_{pe}/\Omega_e)^2 - (\omega_{pi}/\omega)^2$ [9,10]. However, since we are only interested in power dissipation and current generation, toroidal and azimuthal variations will be averaged out by electrons streaming in and out of the resonance cone. Thus, Eq. (6) will form a model for the radial propagation of the rf wave, so that the total power dissipated by the rf wave is given by $(P_D)_{total} = 4\pi^2 R \int^{\bar{a}} P_D \, rdr$, $\overline{a^2} = a^2(2S^2 - 1)^{1/2}$ is the mean half width of the plasma with shape factor S (S = plasma circumference/$2\pi a$).

In slab geometry, $k_z = n_z \, \omega/c$ is a constant for propagation into a perpendicular density gradient. However, in toroidal geometry n_z varies because it is coupled to other components by the curved magnetic field lines [11]. In general, the variation of n_z is complicated. Fortunately, in typical parameters of present interest ($B_o \sim 7.5$ T, $n_e \sim 10^{20}$ m^{-3}), $\omega_{pe}/\Omega_e < 1$, and the poloidal contribution to the variation of n_z is negligible. Thus we can approximate [11]

$$n_z(r) \simeq n_z(a)(R_0 + a)/(R_0 + r) \tag{10}$$

Under the cold plasma electrostatic model, the dielectric function is given by

$$\varepsilon_R(k,\omega) = 1 - \frac{\omega_{pe}^2}{\omega^2 - \Omega^2}\left(\frac{k_\perp}{k}\right)^2 - \left(\frac{\omega_{pe}}{\omega}\frac{k_z}{k}\right)^2 - \left(\frac{\omega_{pi}}{\omega}\right)^2 \tag{11}$$

where $k^2 = k_\perp^2 + k_z^2$. Setting $\varepsilon_R = 0$ yields the dispersion relation

$$\omega^2 = \frac{1}{2}\left\{\omega_{UH}^2 - \left[\omega_{UH}^4 - 4\Omega_e^2 \omega_{pi}^2\left(1 + \frac{m_i}{m_e}\frac{k_z}{k}\right)\right]^{1/2}\right\} \qquad (12)$$

which gives the Trivielpiece - Gould mode ($\omega = \omega_{pe}\, k_z/k$) at the plasma edge where $\omega \sim \omega_{pe}$. At the plasma center where $\omega << \omega_{pe}$, Eq. (12) gives the lower hybrid wave, with $\omega^2 = \omega_{LH}^2\,(1 + m_i\, k_z^2/m_e k^2)$, $\omega_{UH}^2 = \omega_{pe}^2 + \Omega_e^2$, $\omega_{LH}^2 = \omega_{pi}^2 \,/\, (1 + \omega_{pe}^2/\Omega_e^2)$. The perpendicular group velocity is $\left|v_{g\perp}\right| = \omega_{pe}^2\, \Omega_e^2\, k_\perp\, k_z^2/k^4 \omega \omega_{UH}^2$.

Equation (11) has two roots. Besides the slow wave of Eq. (12), there is the outward propagating fast wave. The parallel refractive index of the slow wave must satisfy certain accessibility conditions, otherwise it will be converted to the fast wave [12]. The accessibility conditions are given in terms of n_{LC}, the lower cut off value of the parallel refractive index of the slow wave,

$$n_z > n_{LC} = (1 - \omega^2/\Omega_e\Omega_i)^{-1/2} \qquad \omega \le \omega_c \qquad (13a)$$

$$n_z > n_{Lc} = \omega_{pe}/\Omega_e + [1 + (\omega_{pe}/\Omega_e)^2(1 - \Omega_e\Omega_i/\omega^2)]^{1/2}\,, \qquad \omega > \omega_c \qquad (13b)$$

where $\omega_c^2 \equiv (\omega_{pe}^2\, \Omega_i/2\Omega_e)\, [(1 + 4\Omega_e^2/\omega_{pe}^2)^{1/2} - 1]$. If ω in Eq. (13a) is replaced by the local lower hybrid frequency, ω_{LH}, then Eq. (13a) becomes $n_z > (1 + \omega_{pe}^2/\Omega_e^2)^{1/2}$ which is the accessibility condition used in Refs. [2] and [3]. This condition is incorrect in the context of the present problem because ω is a constant determined at the wave generator and can be very

different from ω_{LH} which varies as the local plasma density.

Figure 2 shows that in order to generate current efficiently, a small n_z is desirable, and the accessibility condition sets a lower bound for n_z. Equation (13) shows that n_{LC} increases with n_e but decreases with B_o, thus current generation will be more effective with high magnetic field and low plasma densities.

As the lower hybrid wave travels into the hot plasma center, it may suffer linear mode conversion into heavily damped hot ion waves [13]. This process may be favorable for lower hybrid heating purpose because it effectively transfers wave energy to the ions, but it is clearly unfavorable for current generation. Thus, to avoid linear mode conversion, we require that n_z be less than an upper cut off value n_{uc} [13]

$$n_z < n_{Uc} = \frac{c}{2v_{Te}}\left(\frac{\omega^2}{\omega_{pi}^2} + \frac{\omega^2}{\Omega_e\Omega_i} - 1\right)\left(\frac{3}{2}\frac{T_e}{T_i} + \frac{3}{8}\frac{\omega^4}{\Omega_e^2\Omega_i^2}\right)^{-1/2} \qquad (14)$$

To satisfy Eqs. (13) and (14) simultaneously imposes a minimum value on the frequency of the lower hybrid wave i.e., $\omega < \omega_{min}$. For typical parameters of interest in the present case, $\omega_{min} \sim 1.4 - 1.7\ \omega_{LH}(0)$.

Decay of the lower hybrid wave via various types of parametric instabilities may also occur. Besides transfering energy to the heavily damped ion quasi-modes, parametric instabilities would also greatly distort the lower hybrid wave spectrum, and thus have to be avoided for current generation purpose. It has been shown that for tokamak-like plasmas the parametric instability with greatest growth rate occur for rf frequencies in the range of $1 < \omega/\omega_{LH}(0) < 2$ [14]. In the ATC lower hybrid heating experi-

ments, parametric instabilities were observed only for $\omega/\omega_{LH}(0) < 1.9$ [15]. Therefore to avoid parametric instabilities, we pick the rf wave frequency to be twice the central lower hybrid frequency.

The various regions for wave-plasma interaction described above are depicted in Fig. 3. We see in Fig. 3 that n_{LC} decreases with higher B. While n_{UC} decreases with higher T_e as given in Eqs. (13)-(14). Since electron Landau damping is the mechanism responsible for current generation, we choose the operating rf frequency to be in that region.

Figure 4 depicts the variation of the rf wave spectrum as it propagates into a plasma with parabolic density and temperature profiles. It shows that a reasonable current profile can indeed be generated by lower hybrid waves when all propagation characteristics are taken into account. The rf driven current profile is depicted in the insert, which is centrally concentrated except for a slight depression in the middle. To generate enough current for MHD stability with this particular rf spectrum and plasma parameters, 5% of the fusion power has to be regenerated as rf power. With the same plasma parameters, different rf spectra will generate very different current profiles. For example, a broader spectrum with less spectral intensity will result in surface current profiles with higher P_F/P_D ratio.

To obtain Figure 4, the rf spectrum is divided into 100 divisions each in the form of Eq. (3), then Eqs. (4), (6) - (8) are used. The dotted curve gives n_{LC} according to Eq. (13), and the spectral peak is seen to shift to higher n_z according to Eq. (10). The initial increase in $\mathcal{E}_{kz}$ is due to the decrease in $v_{g_\perp}$ as n_e increases with $(1 - \rho)$, where $\rho \equiv r/a$. The decrease of $\mathcal{E}_{kz}$ near plasma center is due to Laudau damping of the wave. As can be

seen from Fig. 4, in order to generate current effectively, a very narrow rf spectrum is required. This would demand careful waveguide design.

This paper considers only the case where the wave-plasma system is already in the steady state, i.e. the plateau in electron distribution is already formed. With a Maxwellian electron distribution, the rf wave will suffer tremendous electron Laudau damping if $n_z T_e^{1/2}(\mathrm{KeV}) \gtrsim 5$. This implies that at pre-steady state conditions wave penetration will be difficult until a plateau in the distribution function is formed. The start up scenario of the steady state reactor, (i.e., the temporal evolution of the electron distribution function, the means by which the rf wave bores its way into the heavily Laudau damped region, the type of current profile which is generated and related MHD stability issues) warrents further study but will not be discussed here.

IV. CHARACTERISTICS OF NEARLY IGNITED PLASMAS

At ignition, the electron and ion energy equations are given by

$$(1 - G_i)P_\alpha + P_D - P_{ec} - P_{cyc} - P_{br} - P_{ei} = 0 \tag{15}$$

$$G_i P_\alpha - P_{ic} + P_{ei} = 0 \tag{16}$$

where P_{ec}, P_{cyc}, P_{br}, P_{ei}, and P_{ic} denotes electron transport loss, cyclotron radiation loss, bremsstrahlung loss, electron-ion energy equilibration, and ion transport loss respectively P_{ec} is determined by the empirical scaling law time [16] and P_{ic} is determined by the neoclassical confinement time. P_α is the alpha power density produced by fusion. G_i is the fraction of alpha energy transfered to the ions. Equations (15) and (16) can be used to describe high Q near ignition conditions.

For a given average electron temperature $\bar{T}_e$, the ion equation (16) can be solved for $\bar{T}_i$, then the electron equation (15) is solved to give the minimum density required for ignition, $\bar{n}_{ign}$. The minimum current required for confinement is determined by MHD stability consideration. If the maximum allowable poloidal beta is given by $\beta_p \leq A = R/a$, then

$$I \geq I_p = acS\left[2\pi\bar{n}_e(\bar{T}_e + \bar{T}_i)/A(1 - \Gamma_\alpha)\right]^{1/2} \tag{17}$$

where Γ_α is the ratio of alpha pressure to the thermal plasma pressure and c the speed of light. The current generated must also be able to confine the alpha particles. Theory shows that in order to confine the alphas the

product of current times aspect ratio must exceed a certain value of IA [17]. A rough estimate of this value for a circular plasma is IA > 7.5 MAmp [17]. In all cases considered for the study, this condition is satisfied.

Figure 5 plots $\bar{T}_i$ and $\bar{n}_{ign}$ as a function of $\bar{T}_e$ for R = 6 m, A = 5, B_o = 7.5 T. Two processes for alpha slowing down are considered. The curves marked "C" give the result for the classical mode in which classical slowing down time for the alphas [18] has been used. In the classical mode $0.1 \leq G_i \leq 0.4$ [19] and $0 \leq \Gamma_\alpha \leq 0.3$ for 5 KeV $\lesssim \bar{T}_e \lesssim$ 30 KeV. The curves marked "A" give the result for a possible mode in which the alphas are slowed down anomalously via velocity space instabilities [6]; in this case it is assumed that the alpha slowing down time is much less than the classical slowing down time. In addition, most of the alpha energy will be deposited with the ions so that $G_i \simeq 1$ and $\Gamma_\alpha \simeq 0$. The anomalous transfer of alpha power to ions facilitates ion-electron temperature decoupling i.e., $\bar{T}_e \ll \bar{T}_i$, which is favorable for current generation.

The plasma density is limited by the ignition criterion on the one side and the plasma pressure on the other, $\bar{n}_{ign} \leq \bar{n}_e \leq \bar{n}_{max}$, with

$$\bar{n}_{max} = \bar{\beta}_t B_o^2 / 8\pi[(1+\Gamma_\alpha)\bar{T}_e + \bar{T}_i] \qquad (18)$$

Where $\bar{\beta}_t$ is the averaged ratio of the plasma kinetic pressure to the magnetic field pressure.

V. CURRENT GENERATION EFFICIENCY IN TOKAMAK REACTOR

An important figure of merit for an rf-driven tokamak reactor is

$$Q \equiv P_F/\bar{P}_D = 1.25\, E_\alpha \bar{n}_e^2 \langle\sigma v\rangle_{DT} \left[2\int_0^1 P_D\, \rho d\rho\right]^{-1} \tag{19}$$

where E_α = 3.5 MeV, $\langle\sigma v\rangle_{DT}$ is the average fusion cross-section, and $2\pi^2\, \overline{Ra^2} P_D$ is the rf power required to generate I_p.

For a given $\bar{T}_e$ and $\bar{n}_e$, the value of Q varies with the plasma profiles. Table 1 shows the effect of density, temperature and current profiles on Q. In general, a more peaked profile will yield a lower Q. This can be understood with reference to Fig. 2. For a given rf phase velocity, it is more efficient to generate current in low temperature plasmas. Thus a more gradual current profile means more current is generated at the colder plasma edge. A more gradual density profile means there are more electrons at the colder edge to carry current. A more gradual temperature profile means a lower central temperature. All these conditions will lead to higher Q. By the same arguement, it can be seen that much less rf power is required to generate the surface currents proposed in Ref. 3. In fact, we find that as much as a factor of 2 improvement in Q over a parabolic current profile can be obtained if all current is generated in the $\rho > 0.7$ region. This result is similar to that obtained by the Ehst [3]. However, because of the question of the stability of surface currents, we have only considered centrally peaked current profiles in this study.

We pick the parameters of the high field demonstration power reactor HFCTR [20] as our reference set, $R = 6$ m, $a = 1.2$ m, $B_o = 7.5$ T, $n_e = n_{eo}(1 - \rho^3)$, $T_e = T_{eo}(1 - \rho^2)$, $T_i = T_{io}(1 - \rho^2)$. We will use in our model $B_t = B_o/(1 + \rho/A)$, $J = J_o(1 - \rho^2)$, $2\pi\overline{a^2} \int J\rho d\rho = I_p$. The deuterium-tritium mixture is 50 - 50 and Z_{eff} is taken to be 1. With fixed R, A, $\bar{n}_e$, $\bar{T}_e$, and $\bar{B}_t$, plasma elongation increases I_p, but it also increases the plasma cross section, so that the current density J remains approximately constant. The fusion power density is essentially constant since toroidal beta is limited by propagation requirements rather than by MHD stability requirements. Since Q is determined by the current and power densities, plasma elongation will have little effect on the value of Q. Therefore we will consider a circular reactor when investigating the effects of plasma parameters on Q. Plasma shape factors will be taken into account when we consider total fusion power of the reactor.

Although one may not be able to find a rf spectrum that will generate an exactly parabolic current profile, we have shown in Fig. 4 that a centrally peaked current profile can be generated with a reasonable rf spectrum and a Q value of 20. These values were obtained while simultaneously taking into account the wave propagation effects. Fixing a hypothetical current profile allows a systematic examination of the dependence of Q on various plasma parameters. By setting $\omega = 2\omega_{1h}(0)$, $u_2 = c/n_{LC}v_{Te}$ in Eq. (5) we can find u_1 as a function of ρ and then use Eqs. (19) and (9) to determine Q. Since the maximum of n_{LC} usually occurs at some position $\rho_m \neq 0$, we have let $n_{LC}(\rho < \rho_m) = n_{LC}(\rho_m)$ to insure correct accessibility. In most cases the value of n_z lies in the range $1.2 \lesssim n_z \lesssim 2.0$. Typically $u_2/u_1 \sim 1.06 - 1.2$. Thus a very narrow rf spectrum is required for current

generation, in agreement with the case depicted in Fig. 4.

We have assumed that the rf wave will propagate radially inward from the low magnetic field side of the minor cross section. In general, if we assume wave propagation in the high magnetic field side, i.e., $B_t = B_o/(1 - \rho/A)$, Q will increase by $\sim$ 15%. In reality, the rf wave spirals in following the resonance cone and passes through both the high and low magnetic field sides before reaching the center. However, this complex propagation behavior is not taken into account in our model as discussed in section III. We will adopt the lower Q values obtained with $B_t = B_o/(1 + \rho/A)$ in this study.

Since n_{LC} increases with rf wave frequency ω, Q decreases with ω. The dependence of Q on ω is depicted in Fig. 6, where the circles mark the minimum ω required for penetration into the plasma center as determined by accessibility and linear mode conversion. The crosses in Fig. 6 mark where ω equals twice the center lower hybrid frequency. We have picked $\omega = 2\ \omega_{LH}(0)$ in order to avoid parametric instability. Higher Q can be achieved if lower frequencies can be used. Classical alpha slowing down time is used. (Except for the dashed curve of Fig. 7, all results presented in this paper are for the classical mode).

Figure 7 shows Q as a function of $\bar{T}_e$. The initial rise of Q with $\bar{T}_e$ comes from the rapid increase of P_F with $\bar{T}_i$. The drop of Q with higher $\bar{T}_e$ is caused by the gradual saturation of P_F at high $\bar{T}_i$ coupled with the drop in u_1 with higher $\bar{T}_e$. The maximum Q for the classical mode occurs at around 14 - 15 KeV. The maximum Q obtained in the anomalous mode is $\sim$ 40% more than the maximum Q for the classical mode. This can be explained in

terms of the former's higher $\bar{T}_i$ for more fusion power and lower $\bar{T}_e$, $\bar{n}_{ign}$ for more efficient current generation. Since the anomalous alpha slowing down time is not experimentally verified, we will keep to the lower value of Q resulting from the classical alpha-slowing-down time.

The fusion power P_F scales as n_e^2. The rf power required to generated sufficient current for MHD stability, $P_D I_p/J$, scales as $n_e^{3/2}$. Based on this simple consideration, one would expect $Q \propto n_e^{1/2}$. However, Q is also a rapidly varying function of u, which is limited by the density-dependent n_{LC}. As a result of this implicit dependence, Q is found to decrease with $\bar{n}_e$. Figure 8 shows the variation of Q with $\bar{n}_e$ for $\bar{n}_{ign} \leq \bar{n}_e \leq \bar{n}_{max}$. For a given size reactor, much more fusion power will be produced by operating at higher density at the sacrifice of more rf power recycled. Figure 8 also shows this trade-off between Q and the total fusion power for a circular reactor.

From the discussion of Section III, we see that n_{LC} decreases with higher magnetic field, thus higher Q can be achieved with larger B_o. Figure 9 depict the variations of n_{LC} and Q with B_o for several reactor sizes. Equation (17) shows that the current density required for MHD stability decreases for the larger plasma cross-sectional area, $J_p = I_p/\pi a^2 \propto \sqrt{A}/R$. Since Q is mainly determined by current and power densities, larger reactors (i.e., larger major radius designs) are expected to result in lower current densities and higher Q values. In order to achieve a specific Q value, a trade-off between larger reactor size and higher magnetic field at plasma can be made.

From the above discussion it follows that for fixed $\bar{T}_e$, Q decreases quite rapidly with $\bar{\beta}_t = 8\pi\bar{n}_e(\bar{T}_e + \bar{T}_i)/B_o^2$ as depicted in Figure 10. Current

generation by lower hybrid waves is much more effective in low $\bar{\beta}_t$ reactors. However, since the dependence of Q on B_o^2 is stronger than its dependence on $\bar{n}_e$, for a fixed $\bar{\beta}_t$ larger Q values are obtainable with higher density and higher field. Thus lower hybrid driven steady state current is especially suitable for the high density, high field designs.

Total fusion power of a reactor can be increased by increasing $\bar{n}_e$, R, A, or plasma elongation. We have seen that while higher $\bar{n}_e$ leads to lower Q, elongation leaves Q essentially unchanged, while larger R and larger A will both enhance Q. The total fusion power and the Q of elongated reactors with R = 6 m, and 7 m are given in Figs. 11 and 12. Higher Q values are obtained at lower aspect ratio because for fixed R, the current density required for MHD stability goes as $a^{-1/2} \propto A^{1/2}$. Figures 11 and 12 shows that by choosing different operating densities, various tradeoffs between Q and fusion power can be obtained. With B_o = 7.5 T, S = 1.5, a 2500 MW reactor can adopt a wide range of design parameters, e.g., R = 7 m, A = 3, Q = 31; or R = 7 m, A = 5, Q = 22.5; or R = 6 m, A = 3, Q = 23.5; or R = 6 m, A = 4.5, Q = 18.6, etc. This is very different from the conclusion arrived at Ref. 3 which stated that only large reactors with R > 8 m can produce 2500 MW fusion power with rf-driven centrally peaked current profiles.

VI. CONCLUSIONS

The following considerations regarding the use of rf current generation in tokamak power reactors, based upon present theories for lower hybrid wave properties, have emerged:

The effects of counterstreaming electrons are significant at the elevated temperatures which are typical of reactor operation. These effects significantly reduce the efficiency of rf current generation and reduce the value of $Q = P_{fusion}/P_{rf}$.

Additional effects such as turbulence which might increase the value of n_z in a tokamak would have a very deleterious effect on Q; these effects have occurred in Alcator A at high rf power levels [21].

As a result of accessibility requirements, low values of n_z (needed to obtain high values of Q) are facilitated by operation at lower densities and higher magnetic fields. Consequently Q decreases with increasing values of toroidal beta.

Since Q decreases with increasing plasma density, wall loading and Q must be traded off against each other.

The attainment of high values of $Q(Q \geq 20)$ is quite sensitive to the electron and ion temperatures. High Q operation is facilitated by ion-electron decoupling since the fusion power production depends upon the ion temperature

and the rf power dissipation depends upon the electron temperature. Enhanced ion-electron decoupling by anamolous transfer of the alpha power to the ions can significantly increase the value of Q.

Values of $Q \approx 15 - 30$ may be obtained for moderate size ($R = 6 - 7$ m), high field ($B_o = 7.5$ T), high power density ($\langle P_F \rangle \approx 5 - 10$ MW/m^3) tokamak power reactors.

ACKNOWLEDGMENT

We would like to thank L. Bromberg, J. Fischer, J. Kulp, J. Schultz, and J. J. Schuss for helpful discussions.

REFERENCES:

[1] FISCH, N.J. and BERS, A., in Proc. of the Third Topical Conference on rf Plasma Heating, Pasadena, 1978.

[2] FISCH, N.J. Phys. Rev. Letters 41 (1978) 873.

[3] EHST, D.A., Argonne National Laboratory, ANL/FPP/TM - 120, (1979)

[4] CLARKE, J.F., private communication, (ignition experiment design meeting, Cambridge, MA, Jan., 1979).

[5] BROMBERG, L., COHN, D.R., and FISCHER, J., M.I.T. Plasma Fusion Center Report RR-79-3.

[6] MOLVIG, K., private communication, (ignition experiment design meeting, Cambridge, MA, Jan., 1979)

[7] VEDENOV, A.A., in Review of Plasma Physics, (Consultant Bureau, New York, 1967), Vol. 3.

[8] KARNEY, D.F.F. and FISCH, N.J., Princeton Plasma Physics Laboratory Rept. PPRL-1506 (1979).

[9] BRIGGS, R.J. and PARKER, R.R., Phys. Rev. Letters 29 (1972) 852.

[10] BELLAN, P.M. and PORKOLAB, M., Phys. Fluids 17 (1974) 1592.

[11] KULP, J., Ph.D. Thesis, Department of Electrical Engineering, Massachusetts Institute of Technology, 1978.

[12] GLAGOLEV, V.M., Plasma Phys. 14 (1972) 301.

[13] STIX, T.H., Phys. Rev. Letters 15 (1965) 878.

[14] PORKOLAB, M., Phys. Fluids 20 (1977) 2058.

[15] PORKOLAB, M., BERNABEI, S., HOOKE, W.M., MOTLEY, R.W., and NAGASHIMA, T., Phys. Rev. Letters 38 (1977) 230.

[16] COHN, D.R., PARKER, R.R., JASSBY, D.L., Nucl. Fusion 16 (1976) 31; JASSBY, D.L., COHN, D.R., PARKER, R.R., Nucl. Fusion 16 (1976) 1045.

[17] MCALEES, D.G., Oak Ridge National Laboratory Rept. ORNL-TM-4661 (1974).

[18] JASSBY, D.L., in Plasma Heating in Toroidal Devices, Verenna, Italy (1974) 259.

[19] STIX, T.H., Plasma Phys. 14 (1972) 367.

[20] COHN, D.R. et al., M.I.T. Plasma Fusion Center Research Report RR-78-2 and RR-79-2.

[21] SCHUSS, J.J., et al., M.I.T. Plasma Fusion Center Research Report JA-79-4 (1979).

FIGURE CAPTIONS:

1. Ratio of the actual rf-driven current density J to J_f. J_f is the approximation obtained by neglecting counter streaming thermal current.
2. Effectiveness of rf current generation as a function of the normalized wave parallel velocity, $u = v_z/v_{Te}$.
3. Regions of wave-plasma interaction in the parameter space of lower hybrid wave. The solid lines are n_{LC} for $\bar{T}_e$ = 14 KeV and B_o = 7.5 T and 5 T. The dashed lines are n_{UC} for B_o = 7.5 T and $\bar{T}_e$ = 14, 20 KeV [$\bar{n}_e = 10^{20}$ m^{-3}].
4. Variation of the slow wave spectrum as it propagates from the plasma edge (ρ = 1) to the center (ρ = 0). The dashed curve shows n_{LC}. The rf-driven current profile is depicted in the insert. [R = 6 m, A = 5, B_o = 7.5 T, S = 1, $\bar{T}_e$ = 14 KeV, $\bar{T}_i$ = 19 KeV, $\bar{n}_{20}$ = 0.59, $n_e = n_{eo}(1 - \rho^3)$, $T = T_o(1 - \rho^2)$, f = 2.21 GHz, I_p = 2.4 MA, $Q = P_F/P_D$ = 20]. ($\bar{n}_{20} = \bar{n}_e/10^{20}$ m^{-3}).
5. Averaged ion temperature (solid curves) and $\bar{n}_{ign}$ (dashed curves) as a function of $\bar{T}_e$. Curves marked (A) are for classical alpha slowing down and (C) for anomalous alpha slowing down. [R = 6 m, A = 5, B_o = 7.5 T, S = 1].
6. Fusion to rf power ratio as a function of rf frequency for several electron temperatures. The circle marks for each case $\omega = \omega_{min}$ and the cross marks $\omega = 2\omega_{LH}(0)$. [R = 6 m, A = 5, B_o = 7.5 T, S = 1, $\bar{T}_e$ = 15 KeV, $\bar{T}_i$ = 22 KeV, $n = n_{eo}(1 - \rho^3)$, $T = T_o(1 - \rho^2)$, $J = J_o(1 - \rho^2)$, $\bar{n} = \bar{n}_{ign}$].

7. Fusion to rf power ratio versus $\bar{T}_e$. Solid curves: classical alpha-slowing-down; dashed curves: anomalous alpha-slowing-down, a: $\bar{n} = \bar{n}_{ign}$, b: $\bar{n} = \bar{n}_{max}$. [R = 6 m, A = 5, B_o = 7.5 T, S = 1, $n_e = n_{eo}(1 - \rho^3)$, $T = T_o(1 - \rho^2)$, $J = J_o(1 - \rho^2)$, $\omega = 2\omega_{LH}(0)$].

8. Trade-off between Q (solid curves) and total fusion power (dashed curves). [R = 6 m, A = 5, B_o = 7.5 T, S = 1, $\bar{T}_e$ = 15 KeV, $\bar{T}_i$ = 22 KeV $n_e = n_{eo}(1 - \rho^3)$, $T = T_o(1 - \rho^2)$, $J = J_o(1 - \rho^2)$, $\omega = 2\omega_{LH}(0)$].

9. Accessibility condition of the lower hybrid wave, n_{LC}, as a function of magnetic field (dashed curves). The solid curves give the corresponding fusion to rf power ratio for several size reactors. [A = 5, S = 1 , $n_e = n_{eo}(1 - \rho^3)$, $T = T_o(1 - \rho^2)$, $J = J_o(1 - \rho^2)$, $\bar{T}_e$ = 15 KeV, $\bar{T}_i$ = 22 KeV, $\bar{n}_{20}$ = 0.57, $\omega = 2\omega_{LH}(0)$].

10. Fusion to rf power ratio versus averaged toroidal beta for several plasma densities. [R = 6 m, A = 3, S = 1, $\bar{T}_e$ = 15 KeV, $\bar{T}_i$ = 22 KeV, $n_e = n_{eo}(1 - \rho^3)$, $T = T_o(1 - \rho^2)$, $J = J_o(1 - \rho^2)$, $\omega = 2\omega_{LH}(0)$].

11. Fusion to rf power ratio (solid curves) and the corresponding and total fusion power (dashed curves) versus aspect ratio for several plasma densities. [R = 6 m, B_o = 7.5 T, S = 1.5, $\bar{T}_e$ = 15 KeV, $\bar{T}_i$ = 22 KeV, $n_e = n_{eo}(1 - \rho^3)$, $T = T_o(1 - \rho^2)$, $J = J_o(1 - \rho^2)$, f = 2.23, 2.52, 2.76 GHz for $\bar{n}_{20}$ = .6, .8, 1.0].

12. Fusion to rf power ratio (solid curves) and the corresponding total fusion power. [R = 7 m, B_o = 7.5 T, S = 1.5, $\bar{T}_e$ = 15 KeV, $\bar{T}_i$ = 22 KeV, $n_e = n_{eo}(1 - \rho^3)$, $T = T_o(1 - \rho^2)$, $J = J_o(1 - \rho^2)$, f = 2.23, 2.38, 2.52 GHz for $\bar{n}_{20}$ = .6, .7, .8].

m_n	m_t	m_j	Q
.8	.8	.8	23.2
.8	.8	1	22.6
.8	1	1	22.0
2	.8	1	21.7
1	1	1	21.5
1	1	2	20.4
1	2	1	19.9
2	2	2	16.9

Table 1: Effect of plasma parameter profiles on $Q = P_F / \bar{P}_D$.
$n = n_o(1 - \rho^2)^{m_n}$, $T = T_o (1 - \rho^2)^{m_t}$, $J = J_o (1 - \rho^2)^{m_j}$,
$R = 6m$, $A = 5$, $B_o = 7.5$ T, $S = 1$, $\bar{T}_e = 15$ KeV, $\bar{T}_i = 22$ KeV,
$\bar{n}_{20} = \bar{n}_{ign} = 0.57$.

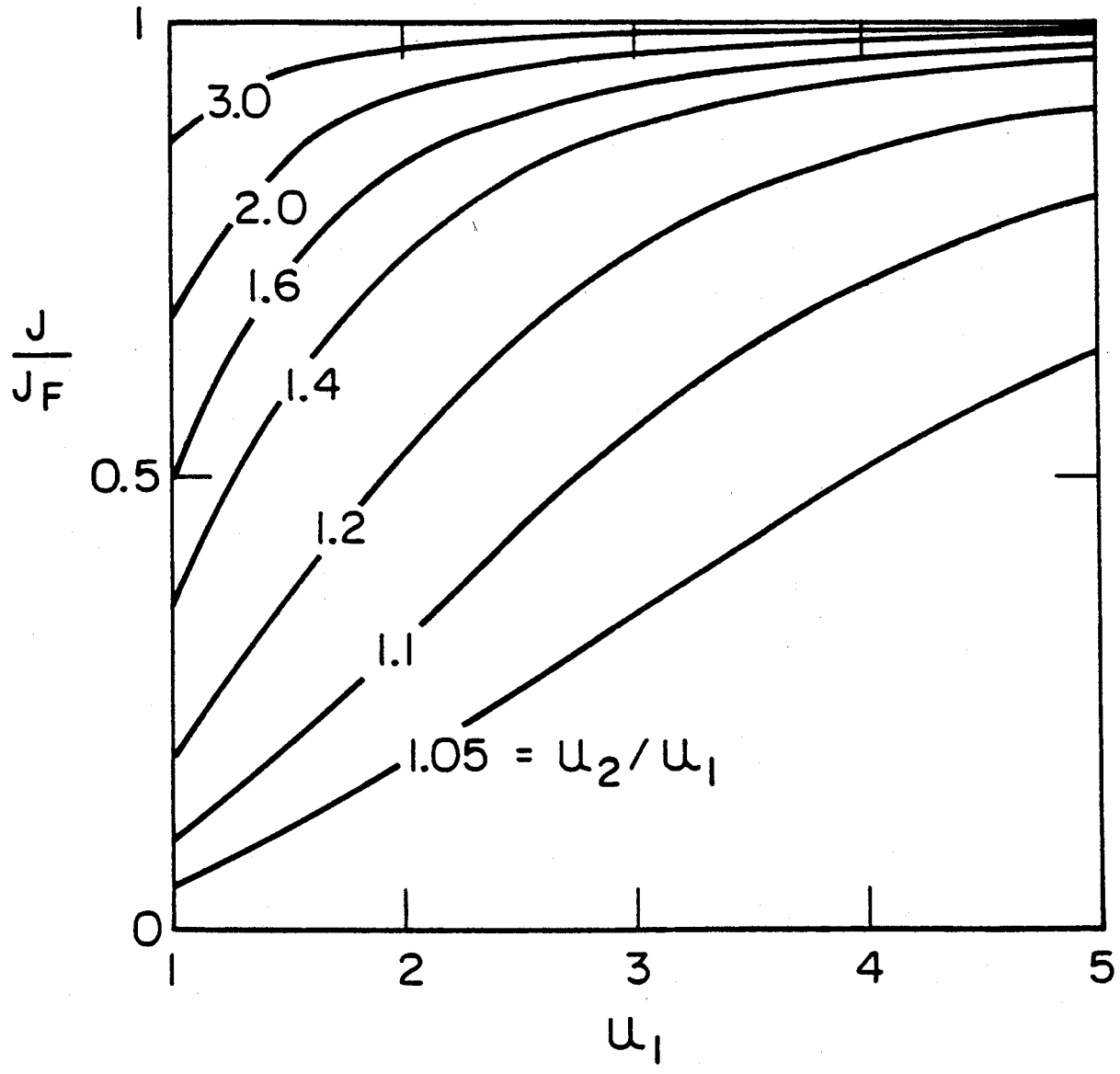

1. Ratio of the actual rf driven current denstiy J to J_F. J_f is the approximation obtained by neglecting counter streaming thermal current.

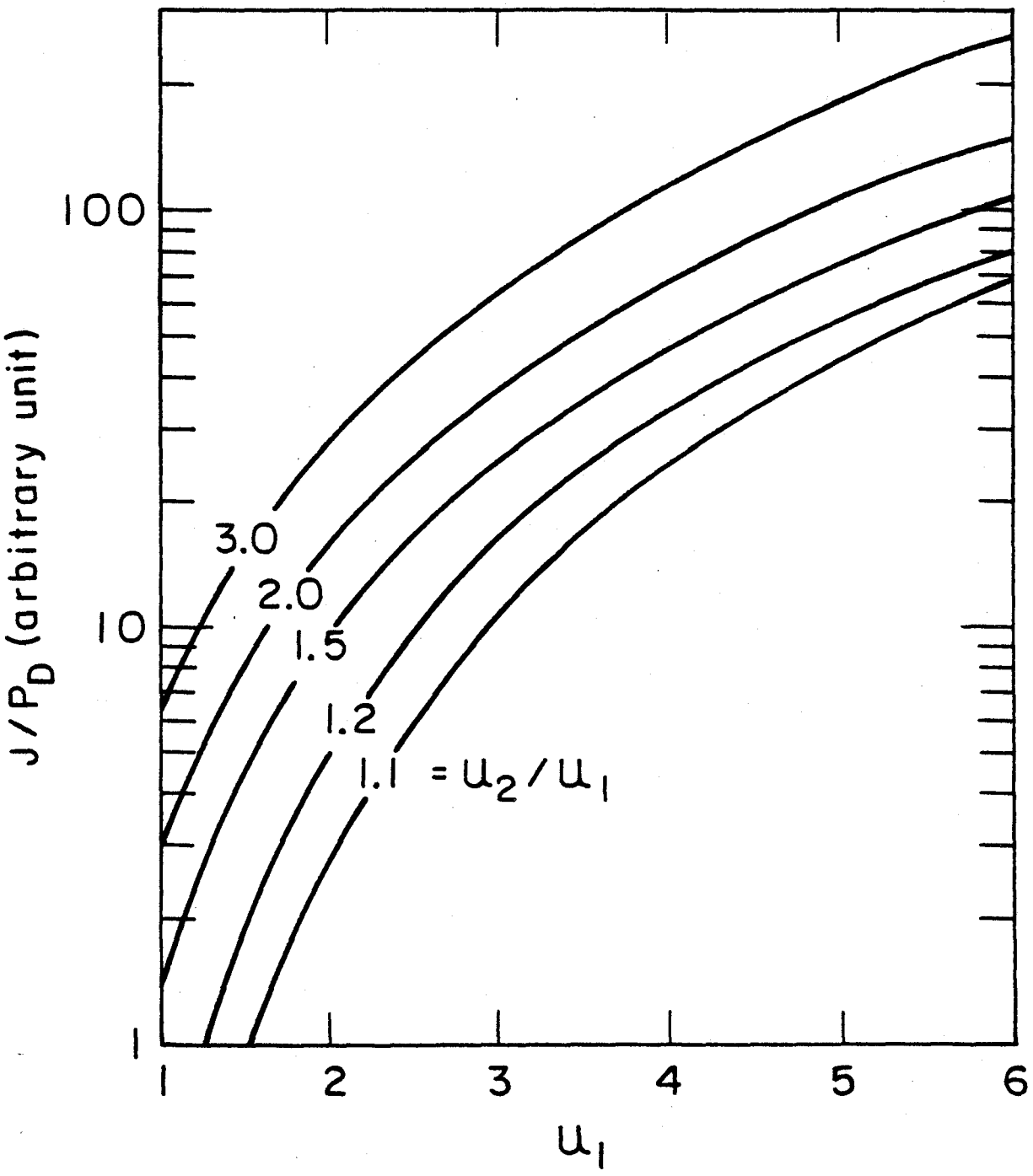

2. Effectiveness of rf current generation as a function of the normalized wave parallel velocity, $u = v_z/v_{T_e}$.

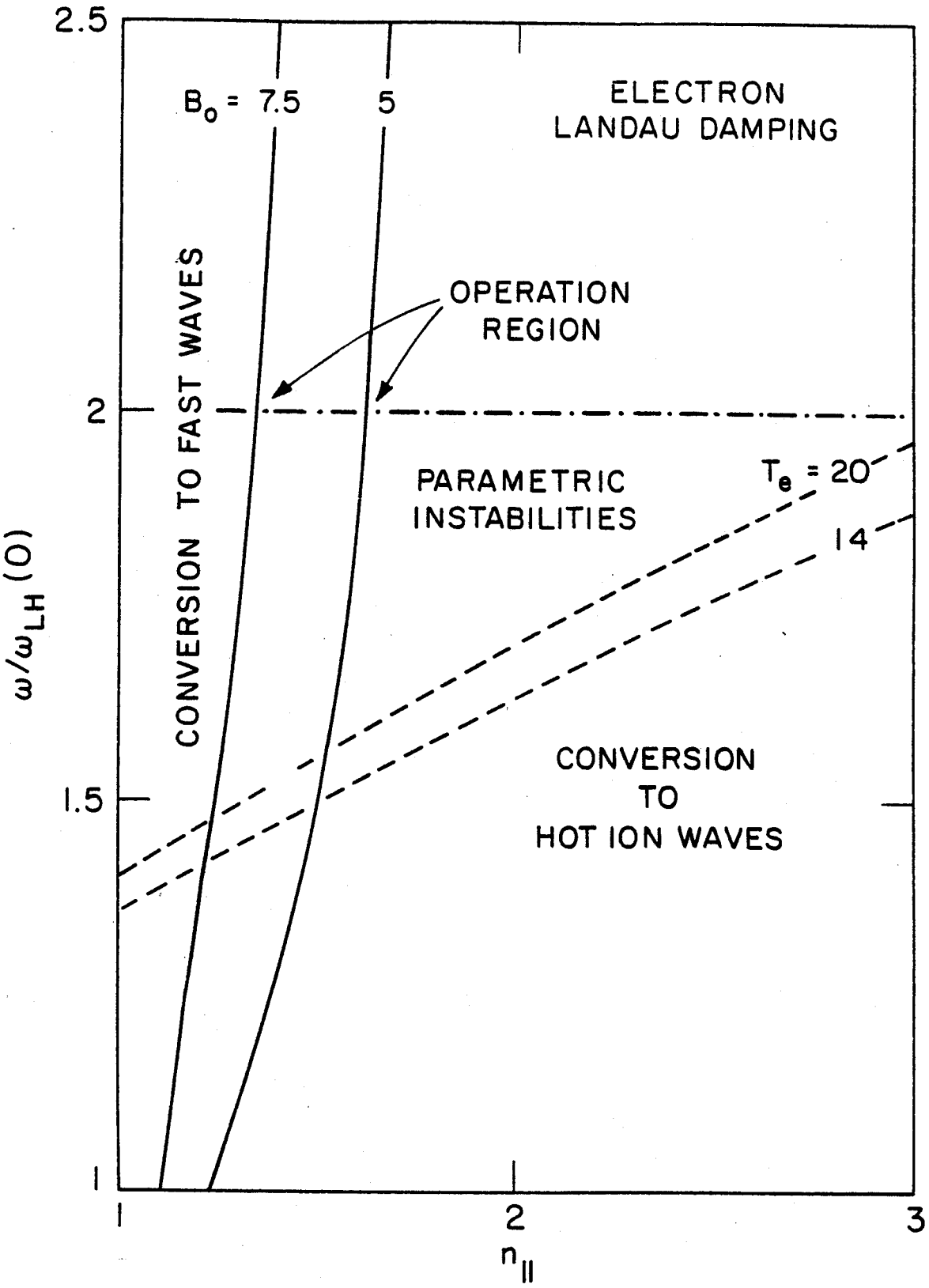

3. Regions of wave-plasma interaction in the parameter space of lower hybrid wave. The solid lines are n_{LC} for $\bar{T}_e$ = 14 KeV and B_o = 7.5, 5T. The dashed lines are n_{UC} for B_o = 7.5 T and $\bar{T}_e$ = 14, 20 KeV [$\bar{n}$ = $10^{20} m^{-3}$].

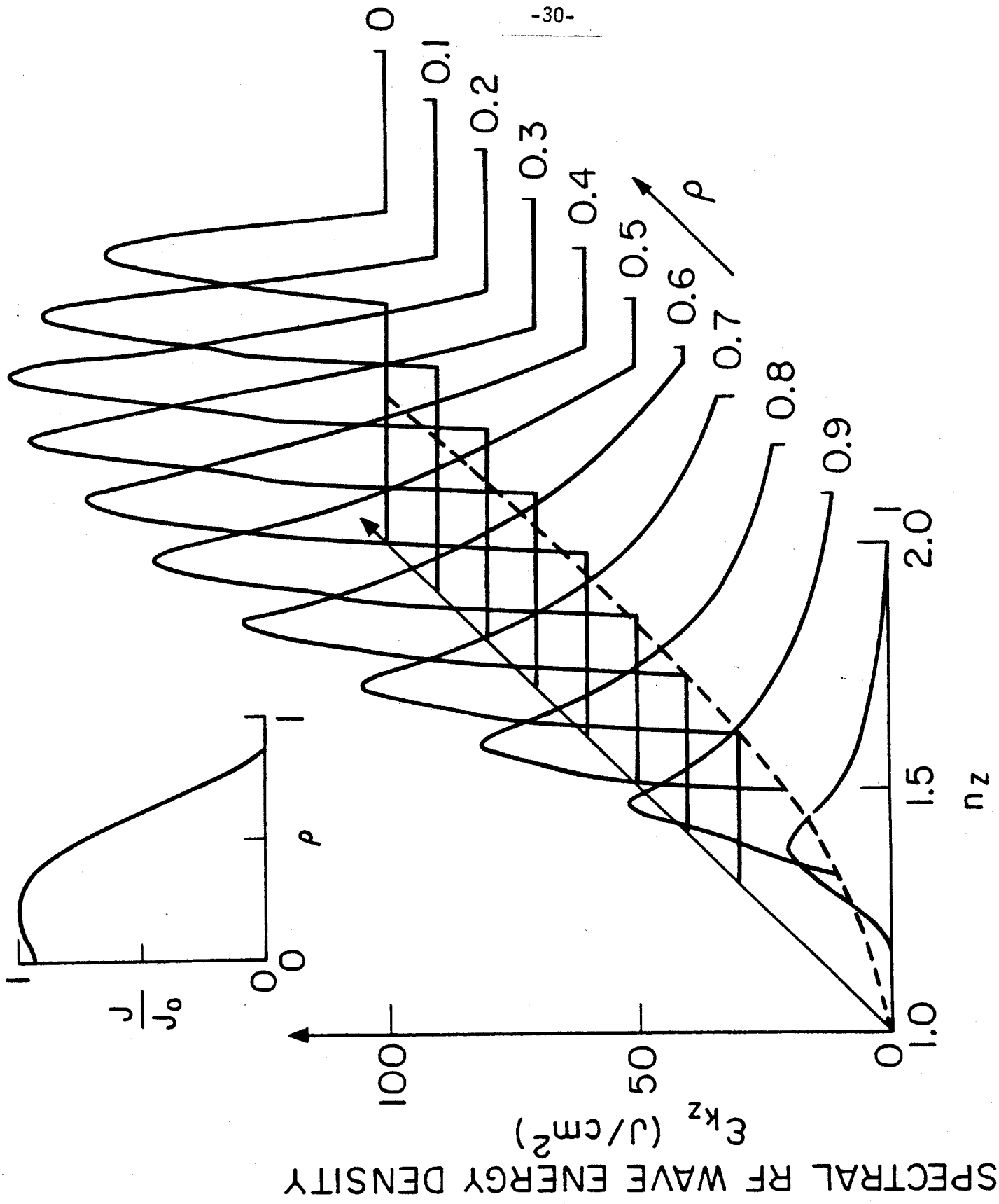

4. Variation of the slow wave spectrum as it propagates from the plasma edge ($\rho = 1$) to the center ($\rho = 0$). The dashed curve shows n_{LC}. The rf-driven current profile is depicted in the insert. [R = 6m, A = 5, B_o = 7.5 T, S = 1, $\bar{T}_e$ = 14 KeV, $\bar{T}_i$ = 19 KeV, $\bar{n}_{20}$ = 0.59, $n_e = n_{eo}(1 - \rho^3)$, $T = T_0(1 - \rho^2)$,

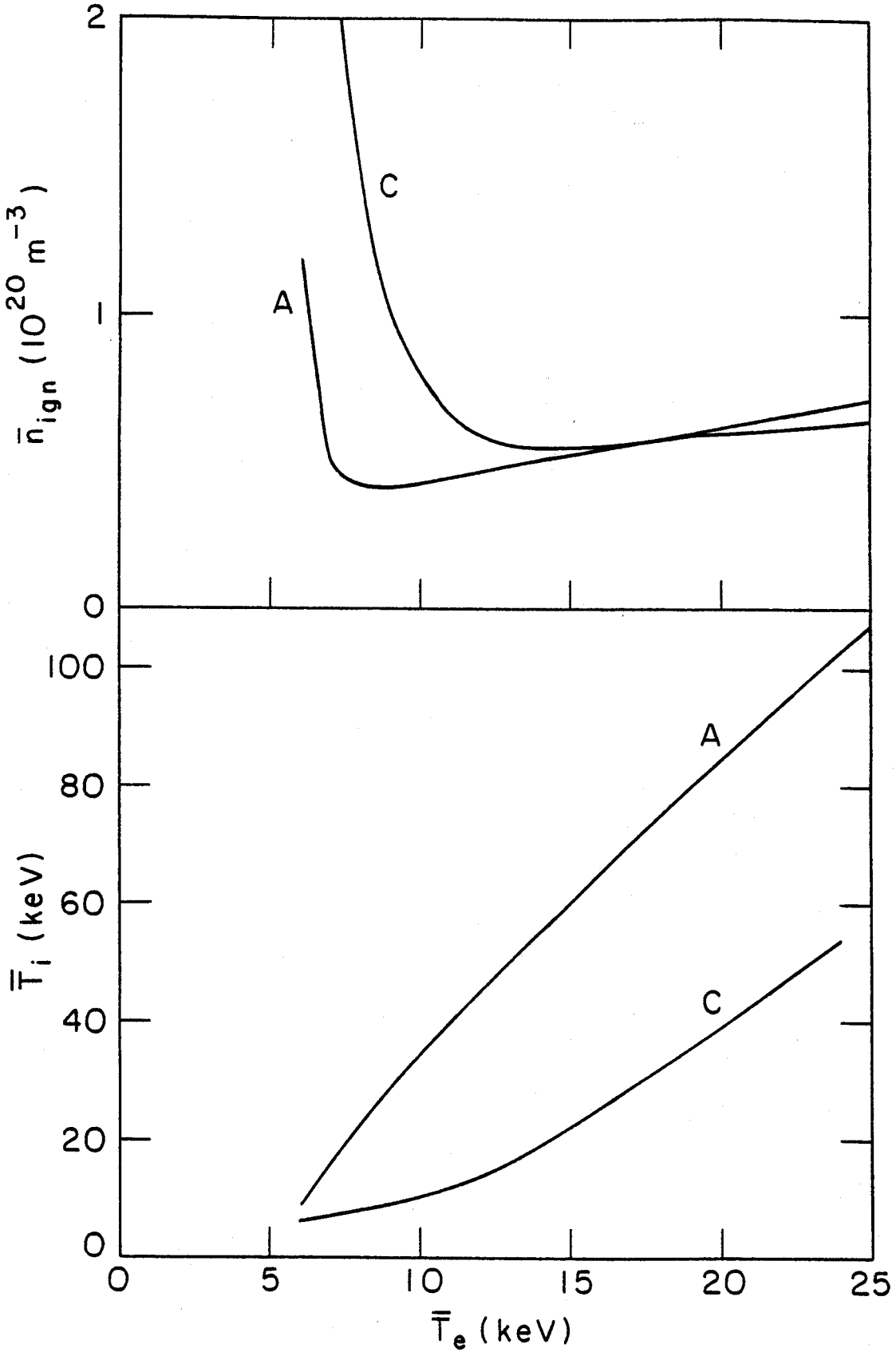

5. Averaged ion temperature (solid curves) and $\bar{n}_{ign}$ (dashed curves) as a function of $\bar{T}_e$. Curves marked (A) are for classical alpha slowing down and (C)

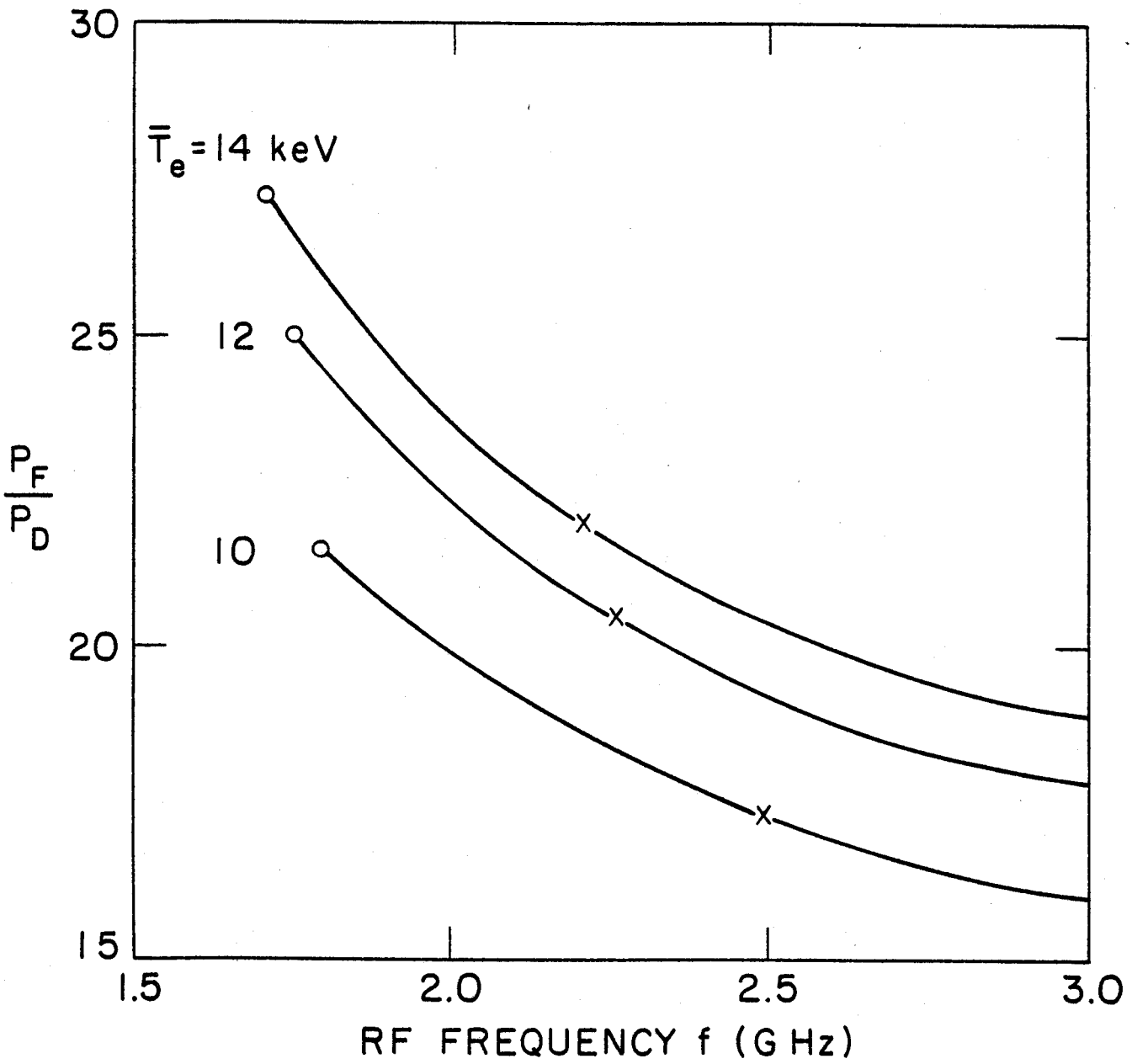

6. Fusion to rf power ratio as a function of rf frequency for several electron temperatures. The circle marks for each case $\omega = \omega_{min}$ and the cross marks $\omega = 2\omega_{LH}(0)$. [R = 6m, A = 5, B_o = 7.5 T, S = 1, $\bar{T}_e$ = 15 KeV, $\bar{T}_i$ = 22 KeV, $n = n_{eo}(1 - \rho^2)$, $T = T_o(1 - \rho^2)$, $J = J_o(1 - \rho^2)$, $\bar{n} = \bar{n}_{ign}$].

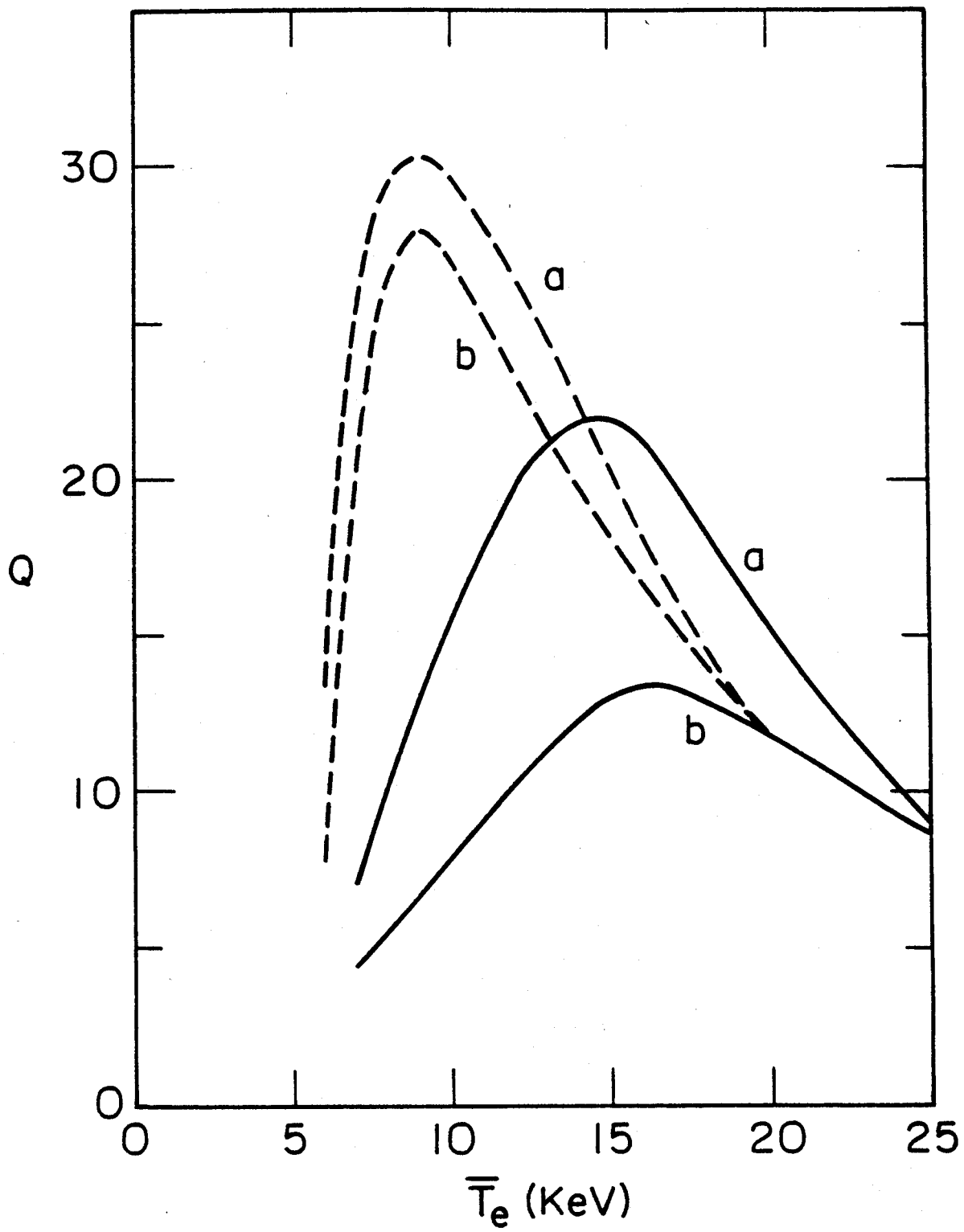

7. Fusion to rf power ratio versus $\bar{T}_e$. Solid curves: classical alpha-slowing-down; dashed curves: anomalous alpha-slowing-down, a: $\bar{n} = \bar{n}_{ign}$, b: $\bar{n} = \bar{n}_{max}$ [R = 6m, A = 5, $\mathfrak{B}_o$ = 7.5 T, S = 1, $n_e = n_{eo}(1 - \rho^3)$, $T = T_o(1 - \rho^2)$, $J = J_o(1 - \rho^2)$, $\omega = 2\omega_{LH}(0)$].

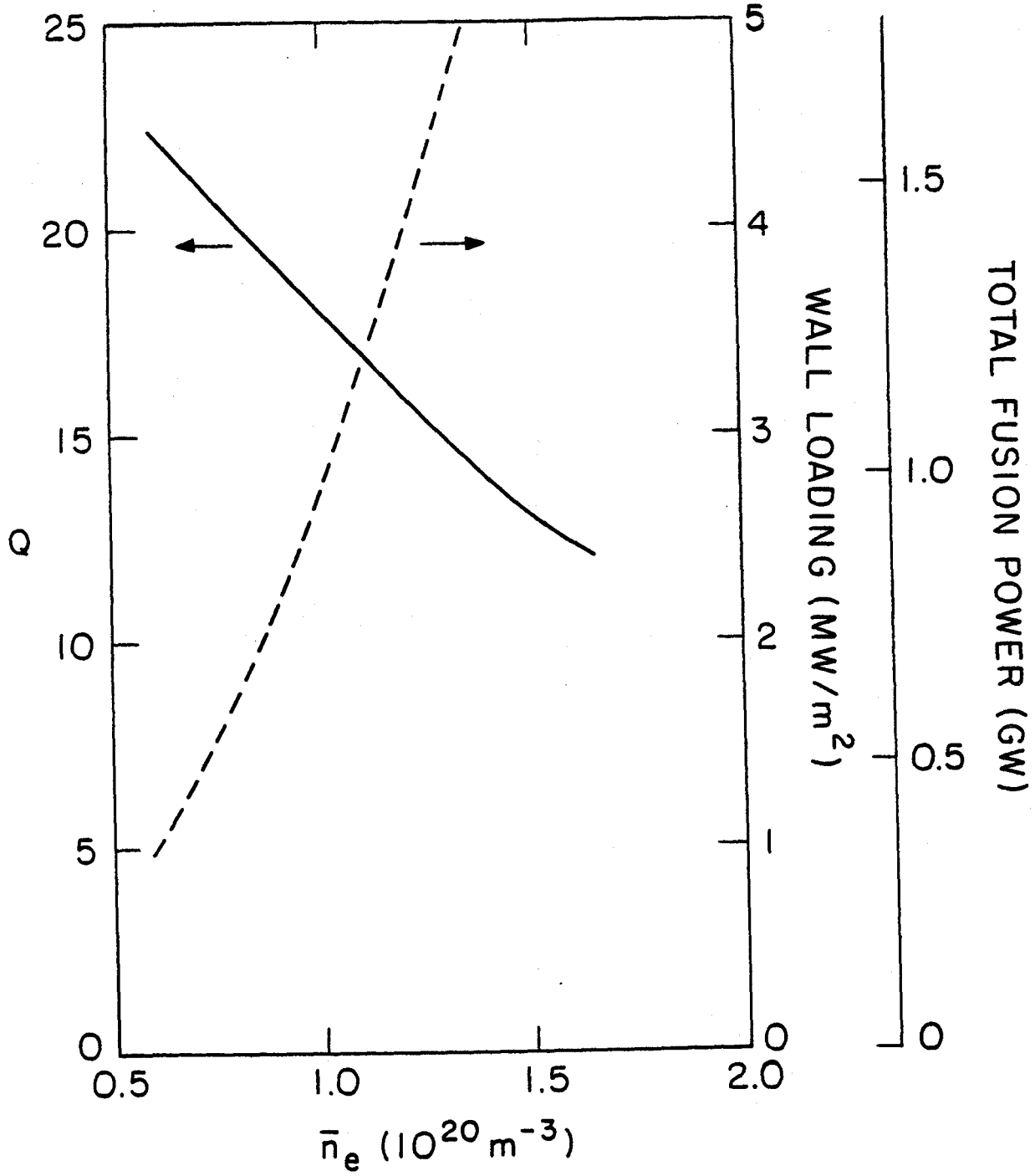

8. Trade-off between Q (solid curves) and total fusion power (dashed curves). [R = 6m, A = 5, B_o = 7.5 T, S = 1, $\bar{T}_e$ = 15 KeV, $\bar{T}_i$ = 22 KeV, $n_e = n_{eo}(1 - \rho^3)$, $T = T_o(1 - \rho^2)$, $J = J_o(1 - \rho^2)$, $\omega = 2\omega_{LH}(0)$].

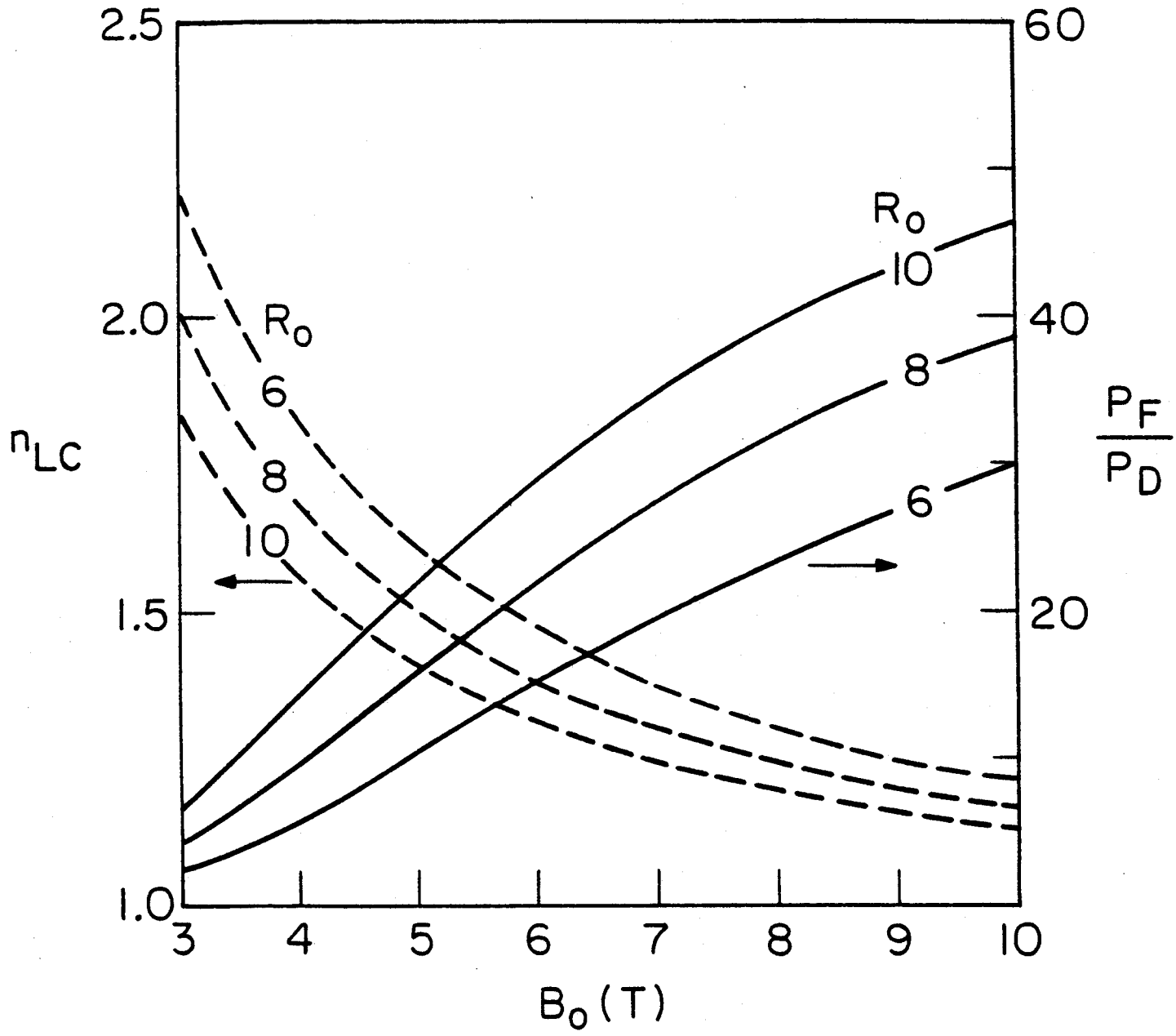

9. Accessibility condition of the lower hybrid wave, n_{LC}, as a function of magnetic field (dashed curves). The solid curves give the corresponding fusion to rf power ratio for several size reactors. [A = 5, S = 1 $n_e = n_{eo}(1 - \rho^3)$, $T = T_o(1 - \rho^2)$, $J = J_o(1 - \rho^2)$, $\bar{T}_e$ = 15 KeV, $\bar{T}_i$ = 22 KeV, $\bar{n}_{20} = 0.57$, $\omega = 2\omega_{i\,H}(0)$].

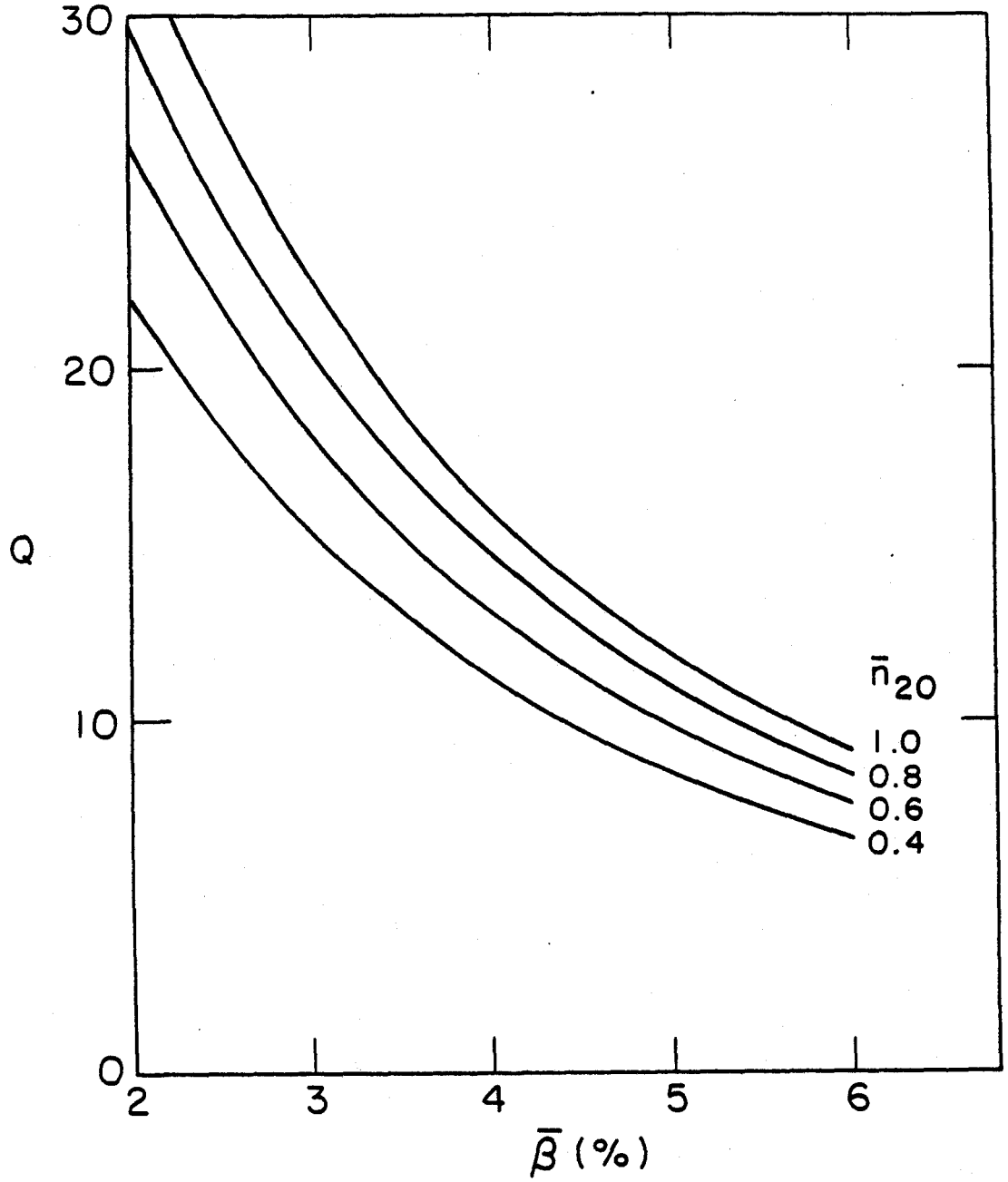

10. Fusion to rf power ratio versus averaged toroidal beta for several plasma densities. [R = 6m, A = 3, S = 1, $\bar{T}_e$ = 15 KeV, $\bar{T}_i$ = 22 KeV, $n_e = n_{eo}(1 - p^3)$, $T = T_o(1 - p^2)$, $J = J_o(1 - p^2)$, $\omega = 2\omega_{LH}(0)$]. $\bar{n}_{20}$ is in units of $2 \times 10^{24} cm^{-3}$.

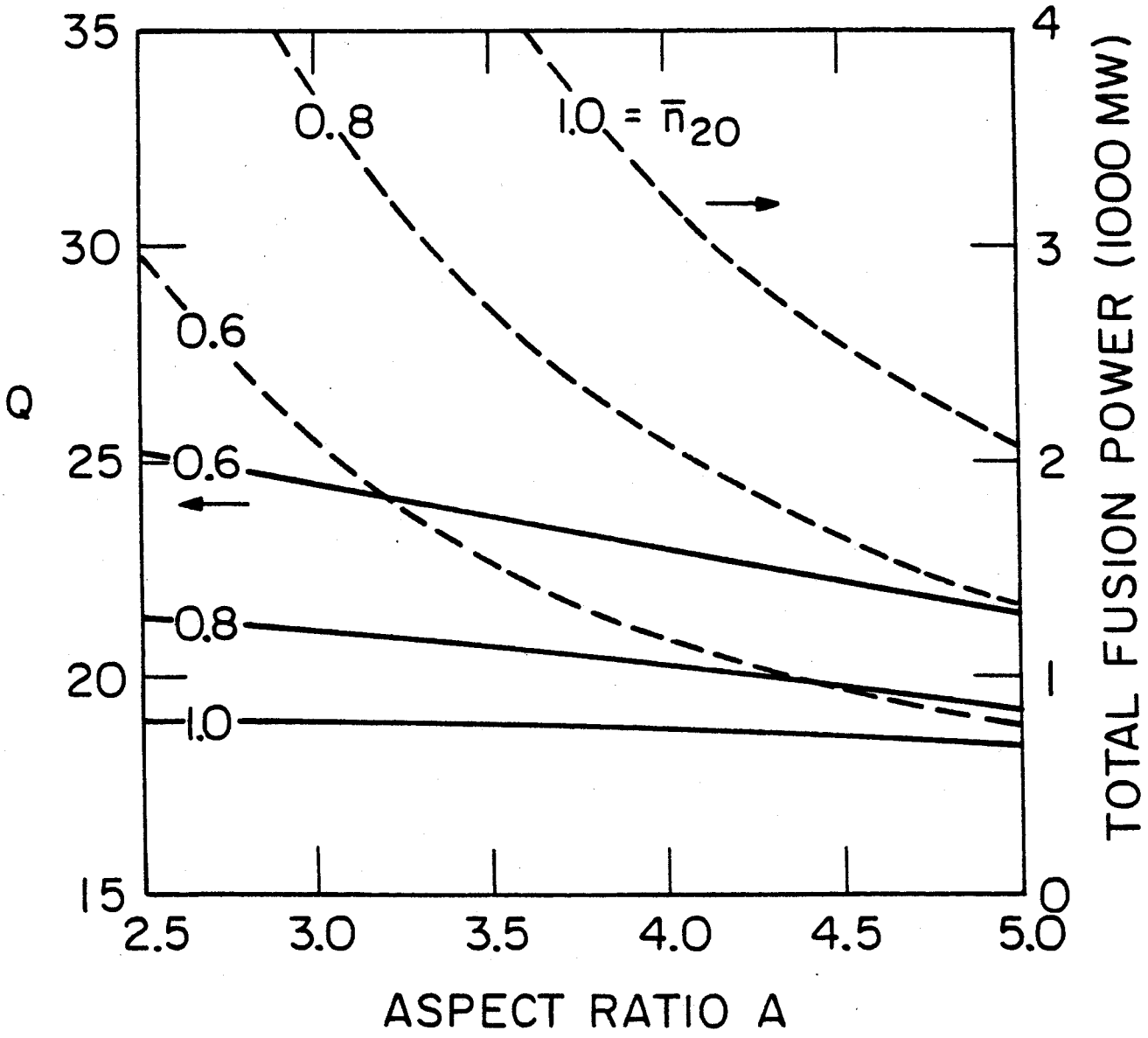

11. Fusion to rf power ratio (solid curves) and the corresponding and total fusion power (dashed curves) versus aspect ratio for several plasma densities. [R = 6m, B_0 = 7.5 T, S = 1.5, $\bar{T}_e$ = 15 KeV, $\bar{T}_i$ = 22 KeV, $n_e = n_{eo}(1 - \rho^3)$, $T = T_o(1 - \rho^2)$, $J = J_o(1 - \rho^2)$, f = 2.23, 2.52, 2.76 GHz for $\bar{n}_{20}$ = .6, .8, 1.0].

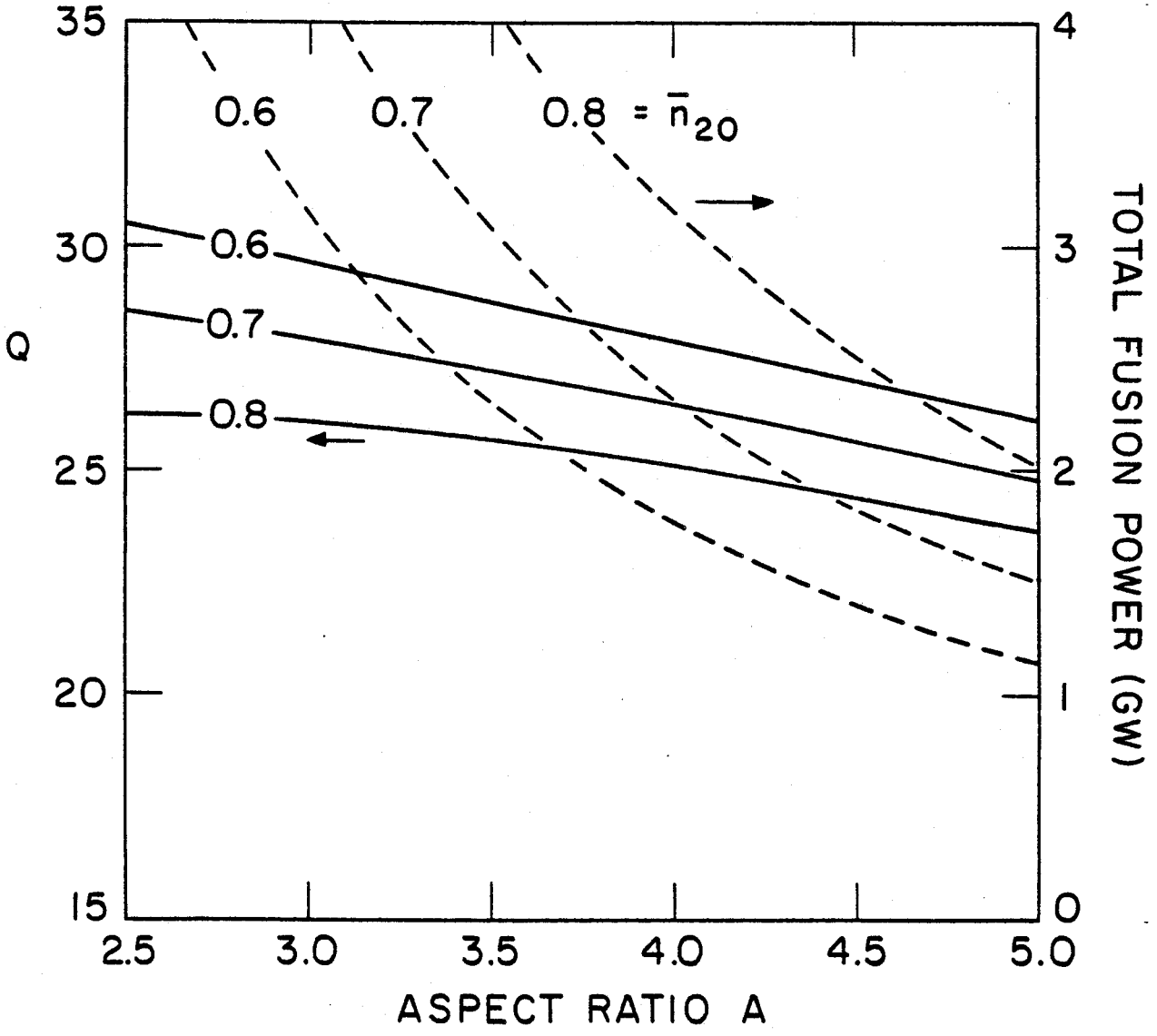

12. Fusion to rf power ratio (solid curves) and the corresponding total fusion power. [R = 7m, B_0 = 7.5 T, S = 1.5, $\bar{T}_e$ = 15 KeV, $\bar{T}_i$ = 22 KeV, $n_e = n_{eo}(1 - \rho^2)$ $T = T_0(1 - \rho^2)$, $J = J_0(1 - \rho^2)$, f = 2.23, 2.38, 2.52 GHz for $\bar{n}_{20}$ = .6, .7, .8].